5G mmWave Downlink Vehicular Positioning

(article starts on next page)

5G mmWave Downlink Vehicular Positioning

Henk Wymeersch[†], Nil Garcia[†], Hyowon Kim[*], Gonzalo Seco-Granados[‡],
Sunwoo Kim[*], Fuxi Wen[†], Markus Fröhle[†]
† Department of Electrical Engineering, Chalmers University of Technology, Sweden
* Department of Electronic Engineering, Hanyang University, Seoul, Korea
‡ Department of Telecommunications and Systems Engineering, Universitat Autonoma de Barcelona, Spain

Abstract—**5G new radio (NR) provides new opportunities for accurate positioning from a single reference station: large bandwidth combined with multiple antennas, at both the base station and user sides, allows for unparalleled angle and delay resolution. Nevertheless, positioning quality is affected by multipath and clock biases. We study, in terms of performance bounds and algorithms, the ability to localize a vehicle in the presence of multipath and unknown user clock bias. We find that when a sufficient number of paths is present, a vehicle can still be localized thanks to redundancy in the geometric constraints. Moreover, the 5G NR signals enable a vehicle to build up a map of the environment.**

I. INTRODUCTION

Vehicles rely on a variety of sensors to localize themselves and build and maintain a (dynamic) map of the environment [1]. Most modern cars are equipped with a GPS receiver, which provides absolute location information, and with a radar sensor providing relative location information with respect to detected objects in the environment. GPS operates by estimating pseudoranges with respect to at least four satellites, and solving a system of equations for the user position and clock bias. The main impairments are blocking of GPS signals due to non-line-of-sight (NLOS) and multipath propagation, as signals are reflected on buildings and other objects [2]. These impairments lead to positioning errors varying from around one meter in ideal conditions to ten meters or more in GPS-challenged areas, such as urban canyons. In contrast, radar sensors explicitly rely on multipath propagation: by measuring the transmitted signal reflected from objects, a radar can determine the relative position (bearing and range) with respect to the sensor coordinate frame [3].

The ability to combine sensing and positioning functionality has recently emerged, mainly in the context of ultra-wide bandwidth communication: with a sufficiently large bandwidth, multipath components become resolvable in the delay domain so that specular paths can be associated with reflectors (or strong scatterers) in the environment [4]. When the locations of reflectors are known, multipath propagation can then help to obtain the position the user. Furthermore, techniques such as simultaneous localization and mapping (SLAM) can be employed to track the user position as well as building up a map of the environment [5], [6]. Conversely, a known user position directly benefits the ability to map the environment. Similar ideas were explored in the context of millimeter-wave communication (mmWave) [7], which will be part of the 5G mobile communication standard. In mmWave,

large antenna arrays at the transmitter and receiver provide a high degree of angular resolvability. This means that multipath components can be estimated not only in terms of delay, but also angle. This idea has led to several works on mmWave positioning, which found that a user can process signals from a single base station in order to (i) determine its own position and orientation; (ii) estimate the reflectors in the environment, provided the base station and user were synchronized [8], [9]. The synchronization assumption can be relaxed when a two-way protocol is executed between the user and base station, though this leads to additional overheads and challenges in both the uplink and downlink beamforming [10]. The use of signal strength ranging combined with direction estimation has been also proposed to avoid the need of synchronization [11], but this causes a performance degradation because the large bandwidth of mmWave is not efficiently used for ranging.

In this paper, we propose to use downlink mmWave signals from a single base station to jointly estimate the vehicle position and orientation, the environment, and the vehicle's clock bias. Thereby, the environment is parametrized by the location of virtual anchors (VA) representing specular reflections and scattering of the transmitted signal on objects. Through a Fisher information analysis, we reveal that multipath propagation is beneficial to estimate the vehicle's clock bias (with respect to the base station), though with some performance penalty compared to a perfectly synchronized scenario. However, in the absence of multipath components, localization of a unsynchronized user using a single base station would be impossible. Moreover, we present a generic downlink positioning system and then analyze specific components of such a system.

II. SYSTEM MODEL AND PROBLEM FORMULATION

A. State Model

We consider a scenario as shown in Fig. 1 with a single static base station (BS), a single mobile user equipment (UE) mounted on a vehicle, and $M - 1$ reflecting surfaces, each parameterized by a point $\mathbf{f}_m$ and a normal vector $\mathbf{u}_m$. The BS is located at $\mathbf{x}_{\mathrm{BS}} = [0, 0, z_{\mathrm{BS}}]^{\mathrm{T}} \in \mathbb{R}^3$, so that with each reflecting surface we can associate a virtual anchor location [12]:

$$\mathbf{x}_{\mathrm{VA},m} = \mathbf{P}_m \mathbf{x}_{\mathrm{BS}} + \mathbf{t}_m, \qquad (1)$$

where $\mathbf{P}_m = \mathbf{I}_3 - 2\mathbf{u}_m \mathbf{u}_m^{\mathrm{T}}$ is a Householder matrix and $\mathbf{t}_m = 2\mathbf{f}_m^{\mathrm{T}} \mathbf{u}_m \mathbf{u}_m$ is a translation vector. Finally, the UE
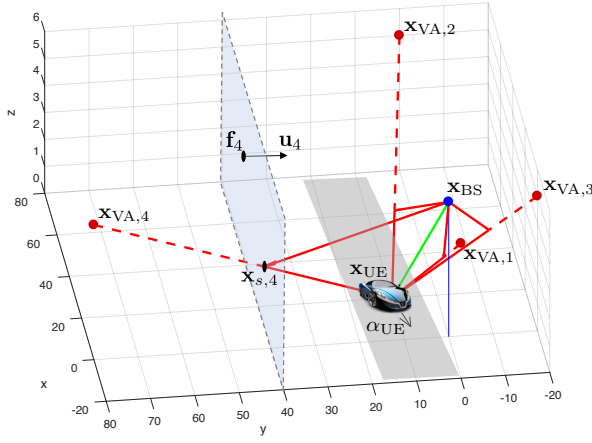
Fig. 1. Scenario with one base station (blue), one vehicle (heading shown with an arrow), and 4 virtual anchors (each corresponding to a vertical wall).

state $\mathbf{s}_k = [\mathbf{x}_{\text{UE},k}^{\text{T}} \, \alpha_{\text{UE},k} \, B_k]^{\text{T}}$ comprises the vehicle's position, orientation (i.e., the vehicle heading since we consider that the vehicle can only rotate around the vertical axis) and clock bias, and it is governed by transition function $p(\mathbf{s}_k|\mathbf{s}_{k-1})$. The epoch duration depends on how frequently the position is updated. We assume the UE has a priori information in a factorized form $p(\mathbf{x}_{\text{VA},m})$, $p(\mathbf{x}_{\text{UE},k})$, $p(\alpha_{\text{UE},k})$ and $p(B_k)$; and demonstrate in Sec. III how this form can be maintained after updating with measurements.

B. Measurement Model

The BS periodically sends a mmWave positioning reference signal (PRS). At epoch k, the received signal at the UE is [13]

$$\mathbf{y}_k(t) = \tag{2}$$
$$\mathbf{W}_k^{\text{H}} \sum_{l=0}^{L_k-1} h_{l,k} \mathbf{a}_{\text{UE}}(\boldsymbol{\theta}_{l,k}) \mathbf{a}_{\text{BS}}^{\text{H}}(\boldsymbol{\phi}_{l,k}) \mathbf{F}_k \mathbf{p}_k(t - \tau_{l,k}) + \mathbf{W}_k^{\text{H}} \mathbf{n}(t),$$

where L_k is the number of resolvable propagation paths, $\mathbf{F}_k$ is a precoder matrix, $\mathbf{p}_k(t)$ the training signal, $\mathbf{W}_k$ a combiner matrix, h_l is a complex channel gain, $\mathbf{a}_{\text{UE}}$ and $\mathbf{a}_{\text{BS}}$ are the antenna response vectors, and $\tau_{l,k}$, $\boldsymbol{\theta}_{l,k}$, and $\boldsymbol{\phi}_{l,k}$ denote time of arrival (TOA), direction of arrival (DOA), and direction of departure (DOD), respectively, of path l at epoch k. Both DOA and DOD have azimuth and elevation components. The AWGN at the receiver is denoted $\mathbf{n}(t)$ and has known power spectral density.

From the observation (2), several techniques exist to recover the triplet of TOA, DOA, and DOD, such as based on sparse recovery [8] or subspace methods [14], which achieve a good balance between estimation accuracy and computational complexity. Assuming that the L_k propagation paths are resolvable in the delay and angular domain, a channel estimation routine provides

$$\mathbf{z}_{l,k} = [\tau_{l,k}, \boldsymbol{\theta}_{l,k}^{\text{T}}, \boldsymbol{\phi}_{l,k}^{\text{T}}]^{\text{T}} + \mathbf{n}_{l,k}, \, l \in \{0, 1, \ldots, L_k - 1\} \tag{3}$$

where $\mathbf{n}_{l,k} \sim \mathcal{N}(\mathbf{0}, \boldsymbol{\Sigma}_{l,k})$, in which $\boldsymbol{\Sigma}_{l,k}$ depends on the channel as well as the precoding, combining, duration of the
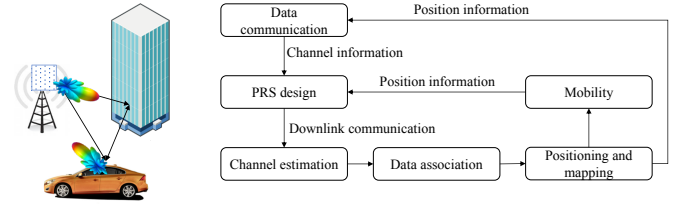

Fig. 2. The stages of 5G mmWave downlink positioning: the vehicle estimates channel parameters from a dedicated PRS (including precoding and combining), which it associates to prior map information and then uses to refine the vehicle position, heading, and clock bias.

training signal, and the receiver. Let the measurement set be $\mathbf{Z}_k = \{\mathbf{z}_{l,k}\}_{l=0}^{L_k-1}$, where the measurements are unordered as explained below.

C. Problem Formulation

Our goal is to determine the marginal posterior distributions $p(\mathbf{x}_{\text{VA},m}|\mathbf{Z}_k)$, $p(\mathbf{x}_{\text{UE},k}|\mathbf{Z}_k)$, $p(\alpha_{\text{UE},k}|\mathbf{Z}_k)$ and $p(B_k|\mathbf{Z}_k)$, given prior distributions on the UE state and possibly some of the VAs. Note that this problem is challenging, due to the unknown clock bias between BS and UE.

III. PROPOSED SOLUTION

In this section, we outline the proposed positioning solution, and display the geometric relations between the channel and the location parameters. Since it is not a priori known which measurement in $\mathbf{Z}_k$ corresponds to which VA source, a sub-optimal method to deal with this data association problem is presented. Finally, the algorithm to solve the positioning and mapping problem via belief propagation on a factor graph is presented.

A. 5G Downlink Positioning

Our solution approach is shown in Fig. 2. First, the mmWave-PRS signals are designed based on prior location information (from the previous epoch, combined with a pre-diction to the current epoch) as well as possibly updated information obtained from channel estimation, required during data transmission. The mmWave-PRS can fill the entire bandwidth in order to localize all users simultaneously[1] and should be designed for sufficient angular coverage. Then, each UE performs channel estimation. Since the estimates of the L_k paths are not yet tied to the M virtual anchors, a data association step must follow. Subsequently, the UE performs positioning and mapping. These estimates can then be provided as inputs for 5G data communication [15]. The mobility model (including a model for the clock) is used to predict the state of the user at the next epoch $k + 1$.

[1]This is essentially an advantage of downlink positioning. In uplink positioning all users could also also transmit their mmWave-PRS simultaneously and use the entire bandwidth; however, the BS would be forced to separate each signal by applying a spatial filter, making the receiver more complex. Nevertheless, the model (3) is still valid, with DOA and DOD switching roles. The analysis, data association and positioning can be applied with only minor modification.

In the following, we will focus on a single epoch and remove the epoch index k, with the understanding that the proposed technique should be combined with a Bayesian filter, such as an extended Kalman filter. Moreover, we will assume that the PRS design and channel estimation are given and limit our discussion to data association and positioning, starting from (3). We are assumed to be provided with (possibly uninformative) prior information about the UE state (in the form $p(\mathbf{x}_{\mathrm{UE}})$, $p(\alpha_{\mathrm{UE}})$, $p(B)$) and prior information regarding some VA (in the form $p(\mathbf{x}_{\mathrm{VA},m})$, $m = 1, \ldots, M$). The number of paths may be greater or smaller than M. First, we will determine the mapping from the location parameters to the channel parameters.

B. Relation Between Channel and Location Parameters

Between each virtual anchor $\mathbf{x}_{\mathrm{VA},m}$ and the user position $\mathbf{x}_{\mathrm{UE}}$, the incidence point of the specular reflection on the reflecting surface is given by the point where the straight line between the VA and UE crosses the reflecting surface (which is itself midway between the BS and the VA), as shown in Fig. 1. It is given by

$$\mathbf{x}_{\mathrm{s},m} = \mathbf{x}_{\mathrm{VA},m} + \frac{(\mathbf{f}_m - \mathbf{x}_{\mathrm{VA},m})^{\mathrm{T}} \mathbf{u}_m}{(\mathbf{x}_{\mathrm{UE}} - \mathbf{x}_{\mathrm{VA},m})^{\mathrm{T}} \mathbf{u}_m} (\mathbf{x}_{\mathrm{UE}} - \mathbf{x}_{\mathrm{VA},m}). \quad (4)$$

Here, $\mathbf{u}_m = (\mathbf{x}_{\mathrm{BS}} - \mathbf{x}_{\mathrm{VA},m})/\|(\mathbf{x}_{\mathrm{BS}} - \mathbf{x}_{\mathrm{VA},m})\|$ and $\mathbf{f}_m = (\mathbf{x}_{\mathrm{BS}} + \mathbf{x}_{\mathrm{VA},m})/2$. Note, this allows to find explicit expressions of $\mathbf{x}_{\mathrm{s},m}$ that only depend on $\mathbf{x}_{\mathrm{VA},m}$, $\mathbf{x}_{\mathrm{BS}}$, and $\mathbf{x}_{\mathrm{UE}}$ (not shown). Next, we state the relations between the channel parameters τ_m, $\boldsymbol{\theta}_m = [\theta_m^{\mathrm{el}}, \theta_m^{\mathrm{az}}]^{\mathrm{T}}$, and $\boldsymbol{\phi}_m = [\phi_m^{\mathrm{el}}, \phi_m^{\mathrm{az}}]^{\mathrm{T}}$ and the system state.

- *Delays:* For the LOS path ($m = 0$), $\tau_0 = \|\mathbf{x}_{\mathrm{BS}} - \mathbf{x}_{\mathrm{UE}}\|/c + B$, where c denotes the speed of light. For a NLOS path $m > 0$, $\tau_m = \|\mathbf{x}_{\mathrm{VA},m} - \mathbf{x}_{\mathrm{UE}}\|/c + B$.[2]
- *Direction of departure:* For the LOS path,

$$\phi_0^{\mathrm{az}} = \arctan\left(\frac{y_{\mathrm{UE}}}{x_{\mathrm{UE}}}\right) \quad (5)$$

$$\phi_0^{\mathrm{el}} = \arcsin\left(\frac{z_{\mathrm{UE}} - z_{\mathrm{BS}}}{\|\mathbf{x}_{\mathrm{UE}} - \mathbf{x}_{\mathrm{BS}}\|}\right), \quad (6)$$

where $\arctan(\cdot)$ is the four-quadrant inverse tangent. Similarly, for the m-th NLOS path

$$\phi_m^{\mathrm{az}} = \arctan\left(\frac{y_{\mathrm{s},m}}{x_{\mathrm{s},m}}\right) \quad (7)$$

$$\phi_m^{\mathrm{el}} = \arcsin\left(\frac{z_{\mathrm{s},m} - z_{\mathrm{BS}}}{\|\mathbf{x}_{\mathrm{s},m} - \mathbf{x}_{\mathrm{BS}}\|}\right). \quad (8)$$

- *Direction of arrival:* Here we note that the DOA is measured in the local frame of reference of the UE, so that the UE orientation must be accounted for. For the LOS path

$$\theta_0^{\mathrm{az}} = \pi + \arctan\left(\frac{y_{\mathrm{UE}}}{x_{\mathrm{UE}}}\right) - \alpha_{\mathrm{UE}} \quad (9)$$

$$\theta_0^{\mathrm{el}} = \arcsin\left(\frac{z_{\mathrm{BS}} - z_{\mathrm{UE}}}{\|\mathbf{x}_{\mathrm{BS}} - \mathbf{x}_{\mathrm{UE}}\|}\right), \quad (10)$$

[2]This is equivalent to $\tau_m = \|\mathbf{x}_{\mathrm{BS}} - \mathbf{x}_{\mathrm{s},m}\|/c + \|\mathbf{x}_{\mathrm{s},m} - \mathbf{x}_{\mathrm{UE}}\|/c + B$.

since the DOA elevation measurement does not depend on the UE orientation, while for the l-th NLOS path

$$\theta_m^{\mathrm{az}} = \arctan\left(\frac{y_{\mathrm{VA},m} - y_{\mathrm{UE}}}{x_{\mathrm{VA},m} - x_{\mathrm{UE}}}\right) - \alpha_{\mathrm{UE}} \quad (11)$$

$$\theta_m^{\mathrm{el}} = \arcsin\left(\frac{z_{\mathrm{VA},m} - z_{\mathrm{UE}}}{\|\mathbf{p}_{\mathrm{VA},m} - \mathbf{p}_{\mathrm{UE}}\|}\right). \quad (12)$$

C. Data Association

Although the channel estimator provides estimates of the parameters TOA, DOA, and DOD of each path, it does not reveal which $\mathbf{z}_l$ corresponds to the LOS path and which $\mathbf{z}_l$ corresponds to which VA. We consider a simple technique based on the global nearest neighbor assignment [16], which provides hard decisions regarding the associations of measurements to VAs.[3] At the current epoch, let M be the number of candidate VAs (including the base station) and L the number of propagation paths (one per observation vector $\mathbf{z}_l$). Each measurement can be explained as coming either from a previously seen VA or as a new VA.[4] We create an $L \times (M+L)$ matrix that captures the corresponding likelihoods:

$$\mathbf{S} = [\mathbf{S}^{\mathrm{D}} \, \beta_{\mathrm{N}} \mathbf{I}_L], \quad (13)$$

where $\mathbf{I}_L$ is an $L \times L$ identity matrix, $\beta_{\mathrm{N}} \geq 0$ is the new target rate and $\mathbf{S}^{\mathrm{D}}$ is an $L \times M$ matrix, with entries

$$[\mathbf{S}^{\mathrm{D}}]_{l,m} = p(\mathbf{z}_l | \mathrm{VA}_m), \quad (14)$$

in which

$$p(\mathbf{z}_l | \mathrm{VA}_m) \approx \mathbb{E}\left\{p(\mathbf{z}_l | \mathbf{x}_{\mathrm{VA},m}, \mathbf{x}_{\mathrm{UE}}, \alpha_{\mathrm{UE}}, B)\right\} \quad (15)$$

$$= \frac{1}{\sqrt{2\pi |\boldsymbol{\Sigma}_l|}} \mathbb{E}\left\{\exp\left(-\frac{1}{2}(\mathbf{z}_l - \boldsymbol{\eta}_m)^{\mathrm{T}} \boldsymbol{\Sigma}_l^{-1} (\mathbf{z}_l - \boldsymbol{\eta}_m)\right)\right\}.$$

Here, $|\boldsymbol{\Sigma}_l|$ is the determinant of $\boldsymbol{\Sigma}_l$, which was defined in (3), and the function $\boldsymbol{\eta}_m(\mathbf{x}_{\mathrm{VA},m}, \mathbf{x}_{\mathrm{UE}}, \alpha_{\mathrm{UE}}, B)$ comprises the TOA, DOA, and DOD computed according to Section III-B from the location of the m-th VA (or base station) and UE state. The expectation in (15) can easily be computed through Monte Carlo integration from the priors. Given the matrix $\mathbf{S}$, we then find an optimal assignment by solving the following optimization problem

$$\text{maximize} \quad \sum_{l=0}^{L-1} \sum_{m=1}^{M+L} x_{l,m} \log S_{l,m} \quad (16a)$$

$$\text{s.t.} \quad x_{l,m} \in \{0, 1\}, \; \forall l, m, \quad (16b)$$

$$\sum_{m=1}^{M+L} x_{l,m} = 1, \; \forall l, \quad (16c)$$

$$\sum_{l=0}^{L-1} x_{l,m} \leq 1, \; \forall m, \quad (16d)$$

which can be solved efficiently with the Kuhn-Munkres algorithm [18], [19]. This approach can determine the LOS path and find new VAs.

[3]A probabilistic/soft data association can also be considered, though this may need modification to the positioning algorithm [17].

[4]False alarms due to clutter and missed detections are not considered, for simplicity.
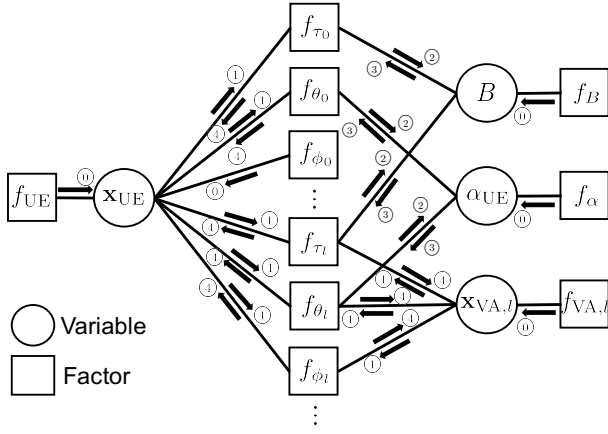
Fig. 3. Factor graph representation of (18) and the message passing schedule. Here, f_X refers either to the prior of state variable X or the likelihood of the estimate of a channel parameter X.

Remark 1. The data association and the localization may be improved by constraining the *joint* probability density function (PDF) of all VA's and the UE state when computing (15). For instance, when $(\mathbf{x}_{\mathrm{UE}} - \mathbf{x}_{\mathrm{s},m})^{\mathrm{T}}(\mathbf{x}_{\mathrm{BS}} - \mathbf{x}_{\mathrm{VA},m}) < 0$ for any m, the UE is on the wrong side of the reflecting surface and the joint PDF would be zero. Since our proposed algorithm (see Section III-D) only provides the *marginal* PDFs, we can account for this by removing samples that violate such constraints. The association could further be extended to account for gating, when measurements are unlikely with respect to the a priori distribution.

D. Positioning and Mapping Algorithm

Once data association has been performed, we have associated with each measurement $\mathbf{z}_l$ either an existing VA, a new VA (with uniform prior), or a false alarm. Assuming no false alarms, we re-order the VA indices to match the measurement indices. The global posterior distribution can then be expressed as

$$p(\mathbf{x}_{\mathrm{UE}}, \alpha_{\mathrm{UE}}, B, \mathbf{x}_{\mathrm{VA},1}, \ldots, \mathbf{x}_{\mathrm{VA},L-1} | \mathbf{Z}) \qquad (17)$$

$$= p(\mathbf{x}_{\mathrm{UE}}) p(\alpha_{\mathrm{UE}}) p(B) \prod_{l=1}^{L-1} p(\mathbf{x}_{\mathrm{VA},l}) \qquad (18)$$

$$\times p(\mathbf{z}_0 | \mathbf{x}_{\mathrm{UE}}, \alpha_{\mathrm{UE}}, B) \prod_{l=1}^{L-1} p(\mathbf{z}_l | \mathbf{x}_{\mathrm{UE}}, \alpha_{\mathrm{UE}}, \mathbf{x}_{\mathrm{VA},l}, B).$$

We make a tacit assumption that factors are removed when needed (e.g., when the data association detects that LOS is not present, the factor with $\mathbf{z}_0$ is removed). We aim to compute the marginal posteriors, which can be achieved by executing belief propagation on a factor graph representation of (18), shown in Fig. 3, where we further approximated $\mathbf{\Sigma}_l$ from (3) to have a diagonal structure.[5] As can be seen, the graph has many cycles, so care needs to be taken when deciding the message passing schedule. In the mmWave regime, we

[5]The proposed technique can be applied, with minor modification, for general $\mathbf{\Sigma}_l$.

consider accurate measurements of the channel parameters, but possibly uninformative priors on clock bias, UE orientation, as well as UE and VA locations. Our proposed message passing schedule is then as follows.

⓪ The LOS DOD and UE position prior are combined into a message $\mu_{\mathbf{x}_{\mathrm{UE}}}(\mathbf{x}_{\mathrm{UE}}) = \mu_{f_{\mathbf{x}_{\mathrm{UE}}} \to \mathbf{x}_{\mathrm{UE}}}(\mathbf{x}_{\mathrm{UE}}) \mu_{f_{\phi_0} \to \mathbf{x}_{\mathrm{UE}}}(\mathbf{x}_{\mathrm{UE}})$. This message captures the knowledge of the UE position based on the LOS DOD (which is always informative, as it is not connected to any other vertex in the graph) and the prior. At the same time all other priors (provided they are informative) send messages to their associated variables (UE bias and orientation, VA position).

① The message $\mu_{\mathbf{x}_{\mathrm{UE}}}(\mathbf{x}_{\mathrm{UE}})$ is sent to all TOA, DOA, DOD likelihoods for all paths (except DOD for LOS path), and the message $\mu_{\mathbf{x}_{\mathrm{VA},l}}(\mathbf{x}_{\mathrm{VA},l})$ is sent to TOA, DOA, DOD likelihoods for l-th NLOS path.

② Each likelihood function, except for DOD, sends a message to bias or orientation. For instance, the message from the TOA likelihood $f_{\tau_l}(\mathbf{x}_{\mathrm{UE}}, B, \mathbf{x}_{\mathrm{VA},l})$ to B is given by

$$\mu_{f_{\tau_l} \to B}(B) = \int \mu_{\mathbf{x}_{\mathrm{UE}}}(\mathbf{x}_{\mathrm{UE}}) \mu_{\mathbf{x}_{\mathrm{VA},l} \to f_{\tau_l}}(\mathbf{x}_{\mathrm{VA},l})$$
$$\times f_{\tau_l}(\mathbf{x}_{\mathrm{UE}}, B, \mathbf{x}_{\mathrm{VA},l}) \mathrm{d}\!\sim\! \{B\}, \qquad (19)$$

where $\mathrm{d}\!\sim\! \{B\}$ denotes integration over all variables except B.

③ Now the bias and orientation have been updated, they can send a message back to the likelihood functions. For instance, the message from B to $f_{\tau_l}(\mathbf{x}_{\mathrm{UE}}, B, \mathbf{x}_{\mathrm{VA},l})$ is given by

$$\mu_{B \to f_{\tau_l}}(B) = p(B) \prod_{l' \neq l} \mu_{f_{\tau_{l'}} \to B}(B). \qquad (20)$$

④ All likelihoods, except for LOS DOD, send messages to the UE position variable, and so do NLOS likelihoods to VA position variable. For instance, the message from $f_{\tau_l}(\mathbf{x}_{\mathrm{UE}}, B, \mathbf{x}_{\mathrm{VA},l})$ to $\mathbf{x}_{\mathrm{UE}}$ is given by

$$\mu_{f_{\tau_l} \to \mathbf{x}_{\mathrm{UE}}}(\mathbf{x}_{\mathrm{UE}}) = \int \mu_{B \to f_{\tau_l}}(B) \qquad (21)$$
$$\times \mu_{\mathbf{x}_{\mathrm{VA},l} \to f_{\tau_l}}(\mathbf{x}_{\mathrm{VA},l}) f_{\tau_l}(\mathbf{x}_{\mathrm{UE}}, B, \mathbf{x}_{\mathrm{VA},l}) \mathrm{d}\!\sim\! \{\mathbf{x}_{\mathrm{UE}}\}.$$

Now, the outgoing messages from the UE position and the VA position towards all the likelihood functions can be computed, so we can go back to step ①.

After a sufficient number of iterations between steps ①–④, the algorithm is stopped and approximate marginal posteriors are found by multiplication of all incoming messages to the associated variables. For instance, for the UE position,

$$p(\mathbf{x}_{\mathrm{UE}} | \mathbf{Z}) \propto p(\mathbf{x}_{\mathrm{UE}}) \prod_{l=0}^{L-1} \mu_{f_{\tau_l} \to \mathbf{x}_{\mathrm{UE}}}(\mathbf{x}_{\mathrm{UE}})$$
$$\times \mu_{f_{\theta_l} \to \mathbf{x}_{\mathrm{UE}}}(\mathbf{x}_{\mathrm{UE}}) \mu_{f_{\phi_l} \to \mathbf{x}_{\mathrm{UE}}}(\mathbf{x}_{\mathrm{UE}}), \qquad (22)$$

and similarly for all the other variables.

IV. FUNDAMENTAL PERFORMANCE ANALYSIS

To gain further understanding in the problem in terms of identifiability and achievable performance, we complement the algorithm description with a Fisher information analysis.

A. Non-Bayesian Case

Consider $\boldsymbol{\zeta} \in \mathbb{R}^{2+3L}$ to comprise all the location parameters (UE position and orientation and clock bias, VA positions), while $\boldsymbol{\eta} \in \mathbb{R}^{5L}$ comprises all the channel parameters. The Fisher information matrix (FIM) of the channel parameters is block diagonal and given by the inverse of the covariance matrix, i.e., $\mathbf{J}(\boldsymbol{\eta}) = \mathrm{blkdiag}\left([\boldsymbol{\Sigma}_l^{-1}]_{l=0}^{L-1}\right)$. The FIM of the location parameters is found by [20]

$$\mathbf{J}(\boldsymbol{\zeta}) = \nabla_{\boldsymbol{\zeta}}^{\mathrm{T}} \boldsymbol{\eta}(\boldsymbol{\zeta}) \mathbf{J}(\boldsymbol{\eta}(\boldsymbol{\zeta}) \nabla_{\boldsymbol{\zeta}} \boldsymbol{\eta}(\boldsymbol{\zeta}), \tag{23}$$

where the Jacobian $[\nabla_{\boldsymbol{\zeta}}(\boldsymbol{\eta}(\boldsymbol{\zeta}))]_{i,j} = \partial[\boldsymbol{\eta}(\boldsymbol{\zeta})]_i/\partial[\boldsymbol{\zeta}]_j$, with the relation $\boldsymbol{\eta}(\boldsymbol{\zeta}))$ previously explicitly described in Section III-B. The computation of the Jacobian is straightforward but tedious, so it is omitted here for brevity. In case $\mathbf{J}(\boldsymbol{\zeta})$ is singular, this means that not all the location parameters are identifiable.

B. The Use of Prior Information

When there is prior information $p(\boldsymbol{\zeta})$ available, we can compute a hybrid FIM for a fixed $\boldsymbol{\zeta}$:

$$\mathbf{J}^{\mathrm{hybrid}}(\boldsymbol{\zeta}) = \mathbf{J}(\boldsymbol{\zeta}) + \mathbf{J}^{\mathrm{prior}}, \tag{24}$$

in which $\mathbf{J}^{\mathrm{prior}}$ comprises the information due to the prior (which is independent on the value of $\boldsymbol{\zeta}$). The FIM in (24) should be interpreted as obtained from receiving sets of two sources of information: one from the channel estimates and one from the prior.[6]

V. RESULTS

A. Simulation Environment

We consider a scenario with 4 vertical walls, a BS at location $[0, 0, 5]^{\mathrm{T}}$ m, a UE at location $[20, 10, 0]^{\mathrm{T}}$ m and 0 degrees orientation. Virtual anchors are placed in locations $[-20, 0, 5]^{\mathrm{T}}$ m, $[80, 0, 5]^{\mathrm{T}}$ m, $[0, -20, 5]^{\mathrm{T}}$ m, and $[0, 80, 5]^{\mathrm{T}}$ m, as depicted in Fig. 1. The measurement covariance matrix is set to diagonal, with 0.1 m standard deviation for TOA estimation, and 0.01 rad standard deviation for angle estimation (both DOA and DOD, azimuth and elevation). In terms of prior information, the UE has location standard deviation of 3.2 meters (only in the horizontal plane, perfect knowledge of the vertical coordinate), while the VA 1, 2, 3 have location standard deviation of 10 meters (also in the horizontal plane), except for the VA 4 at location $[0, 80, 5]^{\mathrm{T}}$ m, for which no prior information is available. We set $\beta_{\mathrm{N}} < \min_{l,m} S_{l,m}^{\mathrm{D}}$, needed for the data association (13).
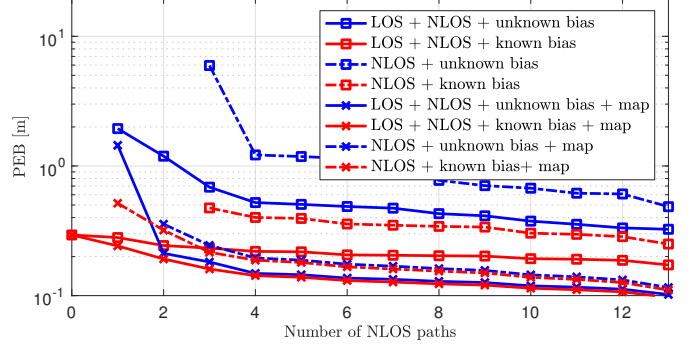

Fig. 4. PEB as a function of the number of NLOS paths for 8 combinations: with and without a LOS path, with and without knowledge of the map (VA positions), and with and without a known clock bias.
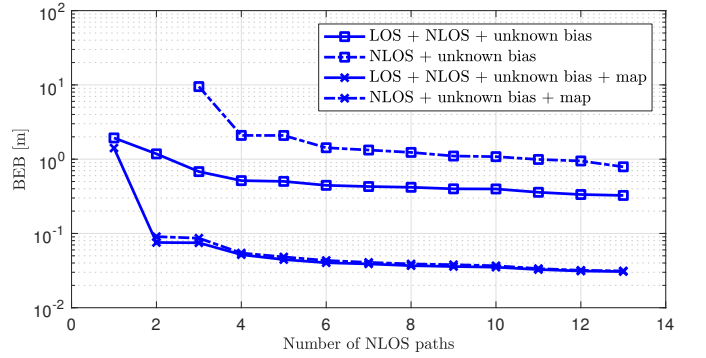

Fig. 5. BEB as a function of the number of NLOS paths for 4 combinations: with and without a LOS path, with and without knowledge of the map (VA positions).
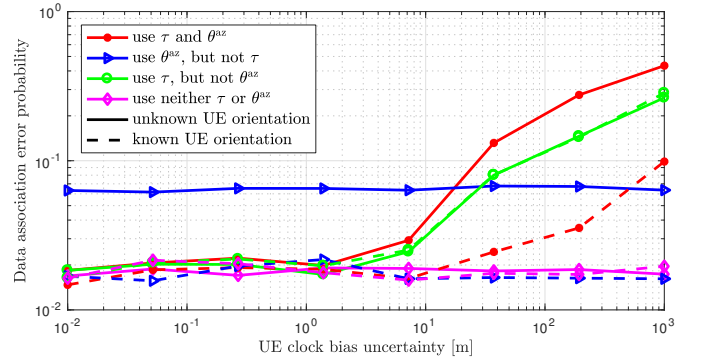

Fig. 6. Data association error probability as a function of the clock bias uncertainty, when different measurements are used in computing the data association likelihood. Full lines corresponding to no a priori knowledge on the UE orientation, while dashed lines correspond to perfect knowledge of the UE orientation.

---

[6]Note that the hybrid FIM characterizes the achievable performance for a deterministic estimation problem, where the unknown parameter $\boldsymbol{\zeta}$ is fixed, and the estimator uses those two sources of information. It is not a Bayesian FIM, which represents the average achievable performance for the ensemble of cases where the parameter values are drawn from the distribution of the prior and the estimator exploits the knowledge of this distribution.
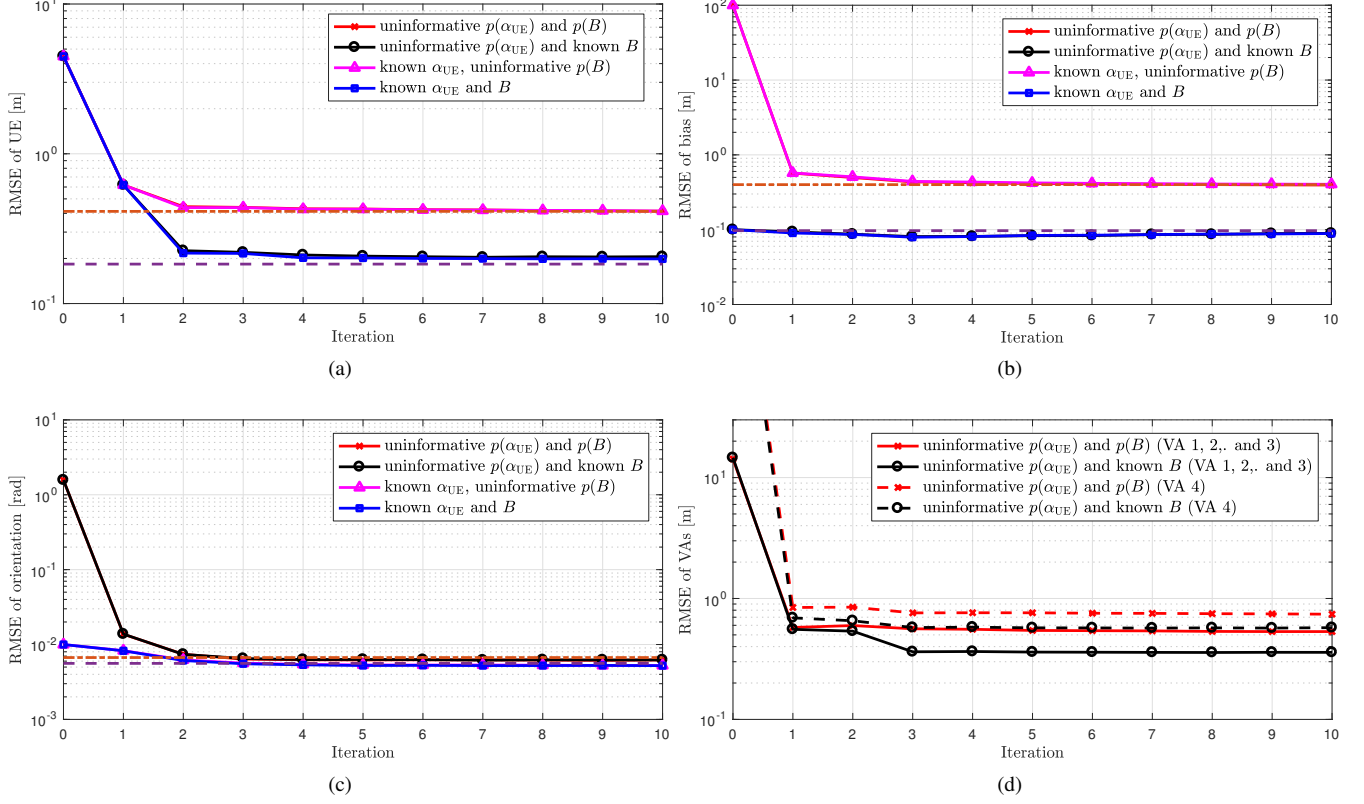
Fig. 7. RMSE as a function of message passing iteration for (a) location of UE, (b) clock bias, (c) UE orientation, (d) locations of VAs. Horizontal lines are the theoretical performance bounds.

B. FIM Analysis

We have studied the identifiability of the positioning problem by considering the scenario above and adding additional virtual anchors (randomly placed). From the inverse of the FIM $\mathbf{J}(\boldsymbol{\eta})$, we can derive several quantities of interest, including the position error bound (PEB), the orientation error bound (OEB), the bias error bound (BEB), and the VA error bound (VAEB), which are lower bounds on the achievable accuracy of the position of the UE, the orientation of the UE, the clock bias of the UE, and the VA position, respectively. The PEB is shown as function of the number of NLOS path in Fig. 4. We observe a number of interesting facts. In all cases, having more paths is beneficial. The best performance is achieved when the both LOS and NLOS paths are available, and when the clock bias and VA positions are known (referred to as "map"), while the worst performance is achieved when only NLOS paths are available, and neither the clock bias nor the VA positions are known. Provided enough paths are available, the system state is always identifiable in spite of the fact that the UE has not a synchronized clock. With an unknown clock bias, one NLOS path is needed when LOS is present. When LOS is not present, at least three NLOS paths are needed, or only two in case map information is available (i.e., the position of the VAs). These results are corroborated by Fig. 5, which clearly confirms that the clock bias can be estimated even with one-way transmission as long as the scenario provides

enough diversity in terms of NLOS paths. In the absence of map information, the PEB for the scenario from Fig. 1 ranges from 2.5 m (NLOS only, unknown bias), over 1 m (LOS and NLOS, unknown bias), to 40 cm (LOS and NLOS, known bias); and the BEB ranges from 2 m (NLOS only, unknown bias) to 0.5 m (LOS and NLOS, unknown bias), while the availability of map information reduces the bounds in one order of magnitude or more.

C. Data Association

Once channel parameter estimates are available, the expectation in (15) is computed using Monte Carlo integration with 1000 samples. We evaluate the data association performance in terms of the data association error probability (i.e., the probability that a measurement is incorrectly assigned) as a function of the a priori uncertainty in the clock bias. The optimization problem (16a) is solved using the Kuhn-Munkres algorithm, which has complexity $\mathcal{O}(L^3)$. Uncertainty in the clock bias and UE orientation affects the TOA measurements and azimuth DOA measurements, respectively. We investigate the impact on the data association when these measurements are included or not in the computation of the data association likelihood. Fig. 6 shows the corresponding results. When the clock bias is known well (i.e., less than 1 meter uncertainty) it is beneficial to include the TOA measurements. However, when the clock bias is highly uncertain, the best performance

is achieved when both TOA and azimuth DOA measurements are ignored. In conclusion, channel parameters that relate to highly uncertain parameters should be avoided during data association.

D. Localization Performance

We study the localization performance after (perfect) data association, using the algorithm described in Section III-D, in four different cases: the prior for the bias B is informative (standard deviation 0.1 m) or uninformative (standard deviation 100 m); the prior for the orientation α_{UE} is informative (standard deviation 0.01 rad) or uninformative (standard deviation $\pi/2$). We use 100 samples for approximating the posterior distributions and perform 10 iterations of message passing. After 200 Monte Carlo runs, we evaluate the root mean squared error (RMSE) of the UE position, the UE bias, the UE orientation, and the VA location, as a function of the iteration index. The results are shown in Fig. 7, including the hybrid bounds derived from (24) (horizontal lines). We observe that in all cases, the algorithm can operate close to the bound and converges after 2 or 3 iterations. It is clearly shown in Fig. 7a that knowing B is in general more beneficial than knowing α_{UE}, as the latter parameter can be accurately estimated from the LOS path, while the former cannot. Fig. 7d demonstrates that having prior information yields better localization accuracy for VA 1–3, compared to VA 4. The final performance under uninformative priors on the clock bias and UE orientation is approximately 40 cm UE error, 40 cm clock bias error (1.3 ns), 0.06 rad orientation error, and 0.6 m (resp. 0.8 m) VA location error for VAs with informative prior (resp. uninformative prior).

VI. Conclusion

5G mmWave signals have unique properties for precise positioning of vehicles and can complement existing on-board sensors. We remove the common assumption of synchronization between vehicle and base station by proposing a framework for joint estimation of the vehicle's position and heading, as well as the clock bias. The method relies on the ability to resolve multipath components and estimate their angles and delays, so as to build up a map of the propagation environment. A Fisher information analysis reveals that the LOS and only one NLOS paths are sufficient to estimate all parameters. In case that the LOS is not present, then three NLOS paths are needed. The performance is also evaluated through a belief propagation method, which is able to attain the performance bounds.

VII. Acknowledgments

References

[1] H. Wymeersch, G. Seco-Granados, G. Destino, D. Dardari, and F. Tufvesson, "5G mm-Wave positioning for vehicular networks," *Wireless Commun. Mag.*, vol. 24, no. 6, pp. 80–86, Dec. 2018.

[2] P. D. Groves and Z. Jiang, "Height aiding, C/N_0 weighting and consistency checking for GNSS NLOS and multipath mitigation in urban areas," *J. Navigat.*, vol. 66, no. 5, pp. 653–669, Sep. 2013.

[3] S. M. Patole, M. Torlak, D. Wang, and M. Ali, "Automotive radars: A review of signal processing techniques," *IEEE Signal Process. Mag.*, vol. 34, no. 2, pp. 22–35, Mar. 2017.

[4] E. Leitinger, P. Meissner, C. Ruedisser, G. Dumphart, and K. Witrisal, "Evaluation of position-related information in multipath components for indoor positioning," *IEEE J. Sel. Areas Commun.*, vol. 33, no. 11, pp. 2313 – 2328, Nov. 2015.

[5] H. Durrant-Whyte and T. Bailey, "Simultaneous localization and mapping: part I," *IEEE Robot. Autom. Mag.*, vol. 13, no. 2, pp. 99–110, Jun. 2006.

[6] E. Leitinger, F. Meyer, F. Tufvesson, and K. Witrisal, "Factor graph based simultaneous localization and mapping using multipath channel information," in *Proc. IEEE ICC-17*, Paris, France, Jun. 2017.

[7] F. Guidi, A. Mariani, A. Guerra, D. Dardari, A. Clemente, and R. D'Errico, "Indoor environment-adaptive mapping with beamsteering massive arrays," *IEEE Transactions on Vehicular Technology*, 2018.

[8] A. Shahmansoori, G. E. Garcia, G. Destino, G. Seco-Granados, and H. Wymeersch, "Position and orientation estimation through millimeter-wave MIMO in 5G systems," *IEEE Trans. Wireless Commun.*, vol. 17, no. 3, pp. 1822–1835, Mar. 2018.

[9] A. Guerra, F. Guidi, and D. Dardari, "Position and orientation error bound for wideband massive antenna arrays," in *Proc. IEEE ICC Workshop on Advances in Network Localization and Navigation (ANLN)*, Jun. 2015, pp. 853–858.

[10] D. R. Brown III and H. V. Poor, "Time-slotted round-trip carrier synchronization for distributed beamforming," *IEEE Trans. Signal Process.*, vol. 56, no. 11, pp. 5630–5643, Nov. 2008.

[11] Z. Lin, T. Lv, and P. T. Mathiopoulos, "3-D indoor positioning for millimeter-wave massive MIMO systems," *IEEE Trans. Commun.*, vol. PP, no. 99, pp. 1–1, Jan. 2018.

[12] H. Naseri and V. Koivunen, "Cooperative simultaneous localization and mapping by exploiting multipath propagation," *IEEE Transactions on Signal Processing*, vol. 65, no. 1, pp. 200–211, Jan 2017.

[13] R. W. Heath, N. González-Prelcic, S. Rangan, W. Roh, and A. M. Sayeed, "An overview of signal processing techniques for millimeter wave MIMO systems," *IEEE J. Sel. Topics Signal Process.*, vol. 10, no. 3, pp. 436–453, Apr. 2016.

[14] F. Roemer, M. Haardt, and G. D. Galdo, "Analytical performance assessment of multi-dimensional matrix- and tensor-based ESPRIT-type algorithms," *IEEE Trans. Signal Process.*, vol. 62, no. 10, pp. 2611–2625, May 2014.

[15] R. D. Taranto, S. Muppirisetty, R. Raulefs, D. Slock, T. Svensson, and H. Wymeersch, "Location-aware communications for 5G networks: How location information can improve scalability, latency, and robustness of 5G," *IEEE Signal Processing Magazine*, vol. 31, no. 6, pp. 102–112, Nov 2014.

[16] Y. Bar-Shalom and X.-R. Li, *Multitarget-multisensor tracking: principles and techniques*. YBS, UK, 1995.

[17] F. Meyer, P. Braca, P. Willett, and F. Hlawatsch, "A scalable algorithm for tracking an unknown number of targets using multiple sensors," *IEEE Trans. Signal Process.*, vol. 65, no. 13, pp. 3478–3493, 2017.

[18] J. Munkres, "Algorithms for the assignment and transportation problems," *J. Soc. Indust. Appl. Math.*, vol. 5, no. 1, pp. 32–38, Mar. 1957.

[19] F. Bourgeois and J.-C. Lassalle, "An extension of the munkres algorithm for the assignment problem to rectangular matrices," *Commun. ACM*, vol. 14, no. 12, pp. 802–804, Dec. 1971.

[20] S. Kay, *Fundamentals of Statistical Signal Processing: Estimation Theory*. Prentice Hall Signal Processing Series, 1993.